ACS OMEGA

Open Access

http://pubs.acs.org/journal/acsodf

Article

Green Synthesis of Cerium Oxide Nanoparticles, Characterization, and Their Neuroprotective Effect on Hydrogen Peroxide-Induced Oxidative Injury in Human Neuroblastoma (SH-SY5Y) Cell Line

Madhugiri Gopinath Mamatha, Mohammad Azam Ansari,* M Yasmin Begum, Daruka Prasad B., Adel Al Fatease, Umme Hani, Mohammad N. Alomary, Sumreen Sultana, Shital Manohar Punekar, Nivedika M.B., Thimappa Ramachandrappa Lakshmeesha,* and Tekupalli Ravikiran*

Cite This: *ACS Omega* 2024, 9, 2639−2649

Read Online

ACCESS | Metrics & More | Article Recommendations | Supporting Information

ABSTRACT: Cerium oxide nanoparticles (CeO_2NPs) have a broad scale of applications in the biomedical field due to their excellent physicochemical and catalytic properties. The present study aims to synthesize the CeO_2NPs from *Centella asiatica* (*C. asiatica*) leaf extract, which has been used in Indian traditional medicine for its neuroprotective properties. The CeO_2NPs were characterized by ultraviolet−visible, X-ray diffraction, Fourier transform infrared, Raman spectroscopy, scanning electron microscopy− energy dispersive X-ray spectroscopy, and high-resolution transmission electron microscopy. The antioxidant property was evaluated by 2,2-di (4-*tert*-octyl phenyl)-1-picrylhydrazyl and OH radical assays. The neuroprotective potential was assessed against the oxidative stress (OS) induced by H_2O_2 in the human neuroblastoma (SH-SY5Y) cell line. CeO_2NPs exhibited significant DPPH and OH radical scavenging activity. Our results revealed that CeO_2NPs significantly increased H_2O_2-induced cell viability, decreased lactate dehydrogenase, protein carbonyls, reactive oxygen species generation, apoptosis, and upregulated antioxidant enzyme activity. Our findings suggest that the CeO_2NPs protect the SH-SY5Y cells from OS and apoptosis, which could potentially counter OS-related neurodegenerative disorders.

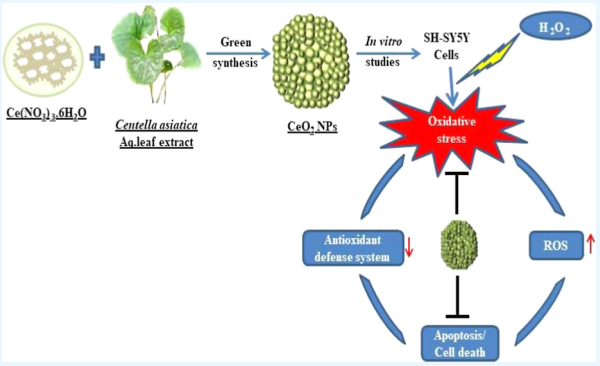

1. INTRODUCTION

Oxidative stress (OS) triggered by reactive oxygen species (ROS) has been implicated in several neurological diseases.[1] ROS, such as hydrogen peroxide (H_2O_2), hydroxyl radicals, and superoxide radicals, are generated in physiological conditions and can cause damage to proteins, lipids, and nucleic acids.[2] H_2O_2 is linked with the production of reactive hydroxyl radicals generated through Fenton's reaction and can promote apoptosis in neuronal cells.[3] Therefore, identifying therapeutic strategies that inhibit ROS generation and apoptosis may be helpful in the intervention and treatment of these OS-linked neurodegenerative diseases. Nanotechnology represents a novel and promising approach due to the unique nanoparticle properties that allow them to penetrate the blood−brain barrier to manage various neurodegenerative disorders.[4] Among them, cerium oxide nanoparticles (CeO_2NPs) play a vital role in a wide range of applications.[5] CeO_2NPs recently gained interest in biological applications due to their potent free radical quenching activity due to the Ce^{3+}/Ce^{4+} redox stoichiometry of the surface.[6] They mimic superoxide dismutase (SOD), catalase (CAT), peroxidase, hydroxyl, and nitric oxide (NO) scavenging properties.[7] Thus, researchers are drawn toward synthesizing nanoparticles (NPs) using biological sources deployed as stabilizing and reducing agents, such as plants, bacteria, and fungus. The synthesis of NPs using plant extract is cost-effective, eco-friendly, fast, and simple.[8]

Medicinal plants traditionally used in ayurvedic medicine have gained recognition worldwide for their antioxidant activity, attributed to the quenching of free radicals.[9] *Centella asiatica* L (*C. asiatica*) is a small creeping perennial herb belonging to the Apiaceae or Umbelliferae family that flourishes in moist and damp areas of India, Indonesia, and other parts of Asia.[10] *C. asiatica* is a natural antioxidant used as a nerve tonic. It is known to exert protective action against age-associated modifications in the brain's antioxidant defense system.[11] Based on this, the present study aimed to synthesize

Received: September 28, 2023
Revised: December 12, 2023
Accepted: December 14, 2023
Published: January 3, 2024

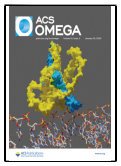

nanoceria using different volumes of *C. asiatica* extract and investigate the neuroprotective potential of H_2O_2-induced OS in SH-SY5Y cells.

2. MATERIALS AND METHODS

2.1. Chemicals and Reagents. Cerium nitrate hexahydrate [$Ce(NO_3)_3{\cdot}6H_2O$], deoxy-2-ribose, 2,2-di (4-*tert*-octyl phenyl)-1-picrylhydrazyl (DPPH), 4′,6-diamidino 2 phenylindole (DAPI), 2′7′ dichlorofluorescein diacetate (DCFH-DA), 2,4-dinitrophenylhydrazine (DNPH), epinephrine, glutathione reductase, reduced glutathione, guanidine hydrochloride, propidium iodide, RNase A, *t*-peroxyhydroxide, thiobarbituric acid, annexin V, and trizol were procured from Sigma (St. Louis, MO, USA). Dulbecco's modified Eagle's medium (DMEM), Ham's F12K mixture, fetal bovine serum (FBS), antibiotic−antimycotic solution, and 3-(4,5-dimethylthiazol-2)-2,5-diphenyl tetrazolium bromide (MTT) were purchased from Himedia chemicals (Mumbai). All solvents were of spectral grade, and other chemicals were of analytical grade.

2.2. Preparation of Aqueous Extract. Fresh leaves of *C. asiatica* were bought from local markets in Bengaluru, India. After washing thoroughly with water, the leaves were shade dried and finely pulverized with a blender. The aqueous extract was made by suspending the powder in warm water. The mixture was kept at room temperature for 24 h and then filtered using Whatman no.1 paper. Further, the filtrate was freeze-dried and stored at −20 °C for further studies.

2.3. Synthesis of CeO_2NPs. The CeO_2NPs were synthesized by solution combustion method according to Lakshmeesha et al.[12] Briefly, various volumes of *C. asiatica* extract (5, 10, 20, and 30 mL) were mixed with the precursor (cerium nitrate hexahydrate) and stirred for 10 min on a magnetic stirrer. The resultant solution was calcined in a preheated muffle furnace at 570 ± 10 °C for 10−20 min.

2.4. Characterization of CeO_2NPs. Fourier transform infrared (FTIR) spectral analysis of the samples was performed using a PerkinElmer FTIR spectrophotometer (Spectrum-1000). The UV−vis spectroscopy was carried out using an SL 159 ELICO UV−vis spectrophotometer. The crystalline nature and phase purity of the NPs were studied using a powder X-ray diffractometer (Shimadzu 7000s). Raman analysis was carried out using a Raman spectrometer (ID Raman reader). The surface morphology was assessed by scanning electron microscopy (SEM) (JEOL JSM 840A) equipped with an energy-dispersive X-ray (EDX) system (Kevex Sigma TM Quasar, USA). The size and selected area diffraction (SAED) patterns were obtained using high-resolution transmission electron microscopy (HR-TEM) (TecnaiG2 20).

2.5. Antioxidant Assays. *2.5.1. DPPH Scavenging Assay.* DPPH assay was performed according to the procedure of Ravikiran et al.[13] 0.5 mL of green synthesized nanoceria were added with 0.1 mM DPPH solution (1 mL) prepared in 95% ethanol and incubated for 20 min at room temperature (RT). The absorbance was recorded at 517 nm against a reagent blank.

$$\text{Scavenging effect (\%)} = \frac{\text{Abs}_{\text{control}(517)} - \text{Abs}_{\text{sample}(517)}}{\text{Abs}_{\text{control}(517)}} \times 100$$

where $\text{Abs}_{\text{control}}$ = absorbance of the control and $\text{Abs}_{\text{sample}}$ = absorbance of the test sample.

2.5.2. Hydroxyl Radical Assay. Hydroxyl radical scavenging assay was performed by the procedure of Halliwell and Gutteridge.[14] 20 μL of various concentrations of the sample were mixed with a reaction mixture composed of 120 μL of deoxyribose (20 mM), phosphate buffer (400 μL, 0.1 M), H_2O_2 (40 μL, 20 mM), $FeSO_4$ (40 μL, 500 mM), and the total volume was made up to 800 μL with distilled water. The reaction mixture was allowed to stand at 37 °C for 30 min, and the reaction was blocked by adding 2.8% trichloroacetic acid (TCA) (0.5 mL) and 0.6% tert-butyl alcohol (TBA) (0.4 mL). Finally, the reaction mixture was placed in a boiling water bath for 20 min. The absorbance was measured at 532 nm.

$$\text{Scavenging effect (\%)} = \frac{\text{Abs}_{\text{control}(532)} - \text{Abs}_{\text{sample}(532)}}{\text{Abs}_{\text{control}(532)}} \times 100$$

where $\text{Abs}_{\text{control}}$ = absorbance of the control and $\text{Abs}_{\text{sample}}$ = absorbance of the test sample.

2.6. In Vitro Studies. *2.6.1. Cell Culture and Treatment.* The SH-SY5Y cells were obtained from the National Centre for Cell Science, Pune. The cells were cultured in 25 cm^3 tissue culture flask (1×10^6 cells/well) in DMEM and Ham's F12 medium (1/1), fortified with 10% FBS, penicillin (100 U/mL), and streptomycin (100 μg/mL). The cells were maintained at 37 °C in a CO_2 incubator, and the medium was replenished every 2−3 days upon attaining 70−80% confluency. The cell viability was assessed after exposure to varying concentrations of H_2O_2 (3.125 to 400 μM) for 24 h to determine the IC_{50} value. The protective effect of the biosynthesized CeO_2NPs on SH-SY5Y cells was estimated by pretreatment with H_2O_2 for a period of 24 h, followed by treatment with different concentrations of nanoceria (10−320 μg/mL) for 24 h. The control cells were also maintained without CeO_2 and H_2O_2 treatment. The cell viability was assessed by MTT assay following the protocol of Mosmann.[15]

2.6.2. MTT Assay. The SH-SY5Y cells were pretreated with H_2O_2 (135 μM) for 24 h, followed by the treatment with CeO_2NPs (10, 20, 40, 80, 160, and 320 μg/mL) for the next 24 h. The cells were then incubated with MTT (5 mg/mL in PBS) for 4 h at 37 °C. The blue formazan crystals that appeared in live cells were solubilized with DMSO. The absorption was recorded at 570 nm in an enzyme-linked immunosorbent assay (ELISA) plate reader (Mode Tecan 1650). The results were expressed as a percentage of the MTT reduction relative to the absorbance of the control cells.

2.6.3. Lactate Dehydrogenase Release Assay. The cytotoxicity was estimated by measuring the lactate dehydrogenase (LDH) release into the culture medium (LDH kit, DIATEK Diagnostics). The cells (SH-SY5Y) were plated in a six-well culture plate (1×10^6 cells/well) and treated with H_2O_2 (135 μM) alone or with CeO_2NPs. After the treatment, the LDH leakage was estimated according to the maker's protocol. The sample absorbance was measured spectrophotometrically at 340 nm, and the LDH leakage was expressed as % LDH release.

2.6.4. Cellular Uptake Studies. The cellular uptake of CeO_2NPs was investigated through flow cytometry analysis following the method of Chauhan et al.[16] The nanoparticle uptake analysis was based on the intensity of the side scatter (SSC) recorded for each cell. The intracellular density of

https://doi.org/10.1021/acsomega.3c07505
ACS Omega 2024, 9, 2639−2649

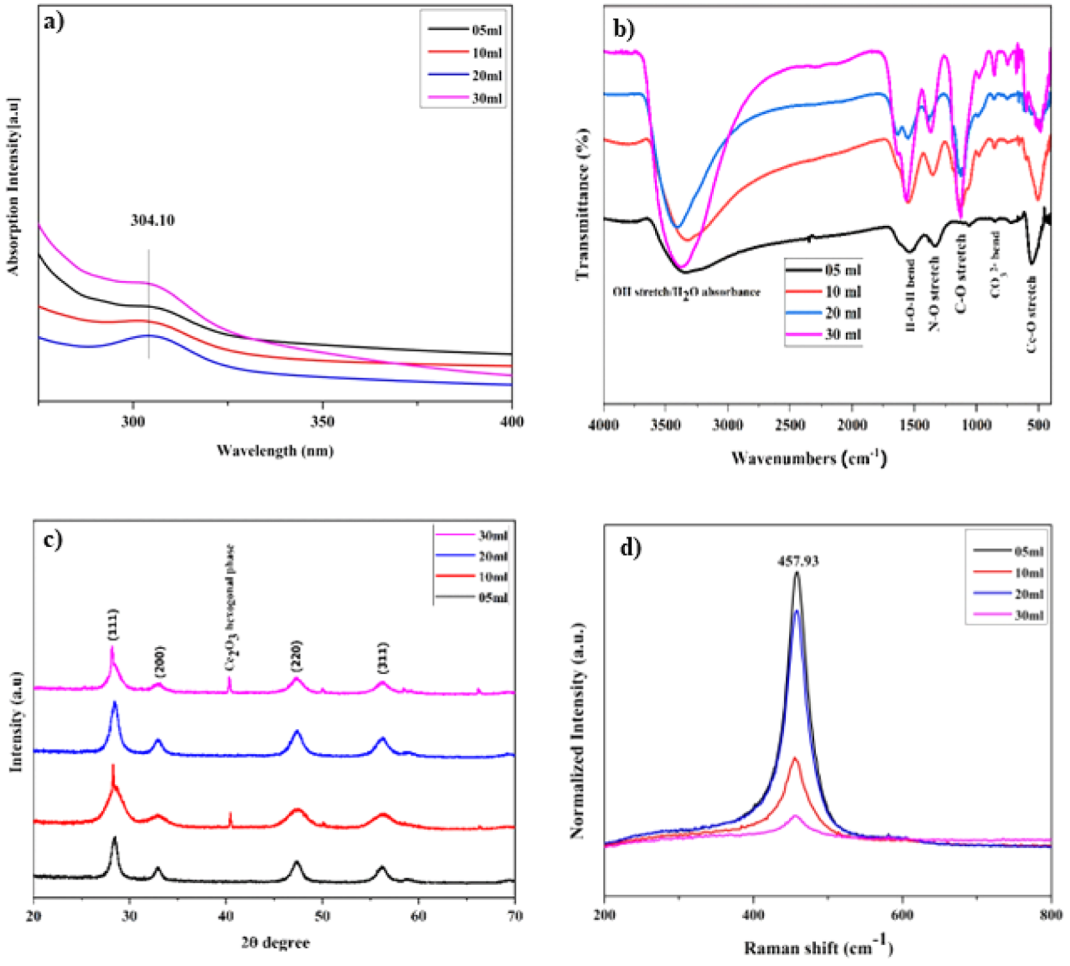

Figure 1. Characterization of CeO_2NPs synthesized using different volumes of *C. asiatica* extract. (a) UV−vis spectroscopy, (b) FTIR, (c) XRD pattern, and (d) Raman spectroscopy.

internalized NPs was directly proportional to the intensity of SSC.

2.6.5. Preparation of Cell Extract. The SH-SY5Y cells were plated in 6-well plates at a density of 1×10^6 cells/well. The cells were pretreated with 135 μM H_2O_2 followed by cell treatment with biosynthesized CeO_2NPs for 24 h. The collected cells were suspended in ice-cold PBS (pH 7.4) and centrifuged at 10,000*g* (Plastocrafts, Superspin RV/FM) at 4 °C for 20 min. The supernatant was utilized to estimate the enzymatic antioxidants and markers of OS. The protein content was estimated by the method of Lowry et al.[17] using bovine serum albumin (BSA).

2.6.6. Measurement of Antioxidant Enzyme Activities. The SOD activity was estimated by the method of Misra and Fridovich.[18] The tissue supernatant (100 μL) was mixed with 880 μL of carbonate buffer (0.05 M, pH 10.2) and ethylenediaminetetraacetic acid (EDTA) (0.1 mM), followed by the addition of 20 μL of epinephrine (30 mM, 0.05% acetic acid). The enzyme activity was estimated by recording the absorbance at 480 nm for 5 min. One unit of enzyme activity is the amount of enzyme that resulted in the inhibition (50%) of epinephrine deterioration.

The determination of CAT activity was performed following the protocol of Aebi.[19] The tissue supernatant (100 μL) was added to an equivalent volume of absolute alcohol and incubated at RT (30 min), followed by triton X-100 addition. The desired amount of this reaction mixture was mixed with an equal volume of H_2O_2 (0.066 M) in phosphate buffer, and the decline in absorbance was recorded for 1 min at 240 nm. The enzyme activity was measured using an extinction coefficient of 43.6 M cm^{-1}. One unit of enzyme activity was equivalent to the moles of H_2O_2 degraded min^{-1} mg^{-1} of protein.

The protocol of Flohe and Gunzler[20] was used to measure glutathione peroxidase (GPx) activity. The reaction mixture contains phosphate buffer (500 μL), 100 μL of reduced glutathione (GSH, 0.01 M), 100 μL of reduced nicotinamide adenine dinucleotide phosphate (NADPH) (1.5 mM), and glutathione reductase (100 μL). The tissue extract (100 μL) was added with a known volume of the reaction mixture and incubated (37 °C for 10 min). After incubation, 50 μL of 12 mM *t*-butyl hydroperoxide was mixed with a tissue reaction mixture (450 μL). The absorbance was noticed at 340 nm for 3 min. The calculation of enzyme activity was done by taking the molar absorption coefficient of 6.229×10^3 M cm^{-1}. A unit of activity equals mM NADPH oxidized/min/mg protein.

2.6.7. Markers of OS. 2.6.7.1. Measurement of Protein Oxidation. Protein carbonyls (PCs) were quantified by the procedure of Levine et al.[21] The supernatant (100 μL) from the tissue extract was incubated with 10 mM (2,4-dinitrophenyl)hydrazine (DNPH) (0.5 mL) in HCl (2 M) in the dark for 60 min. 20% TCA (0.5 mL) was then added to precipitate the protein and centrifuged at 4 °C for 3 min at

https://doi.org/10.1021/acsomega.3c07505
ACS Omega 2024, 9, 2639−2649

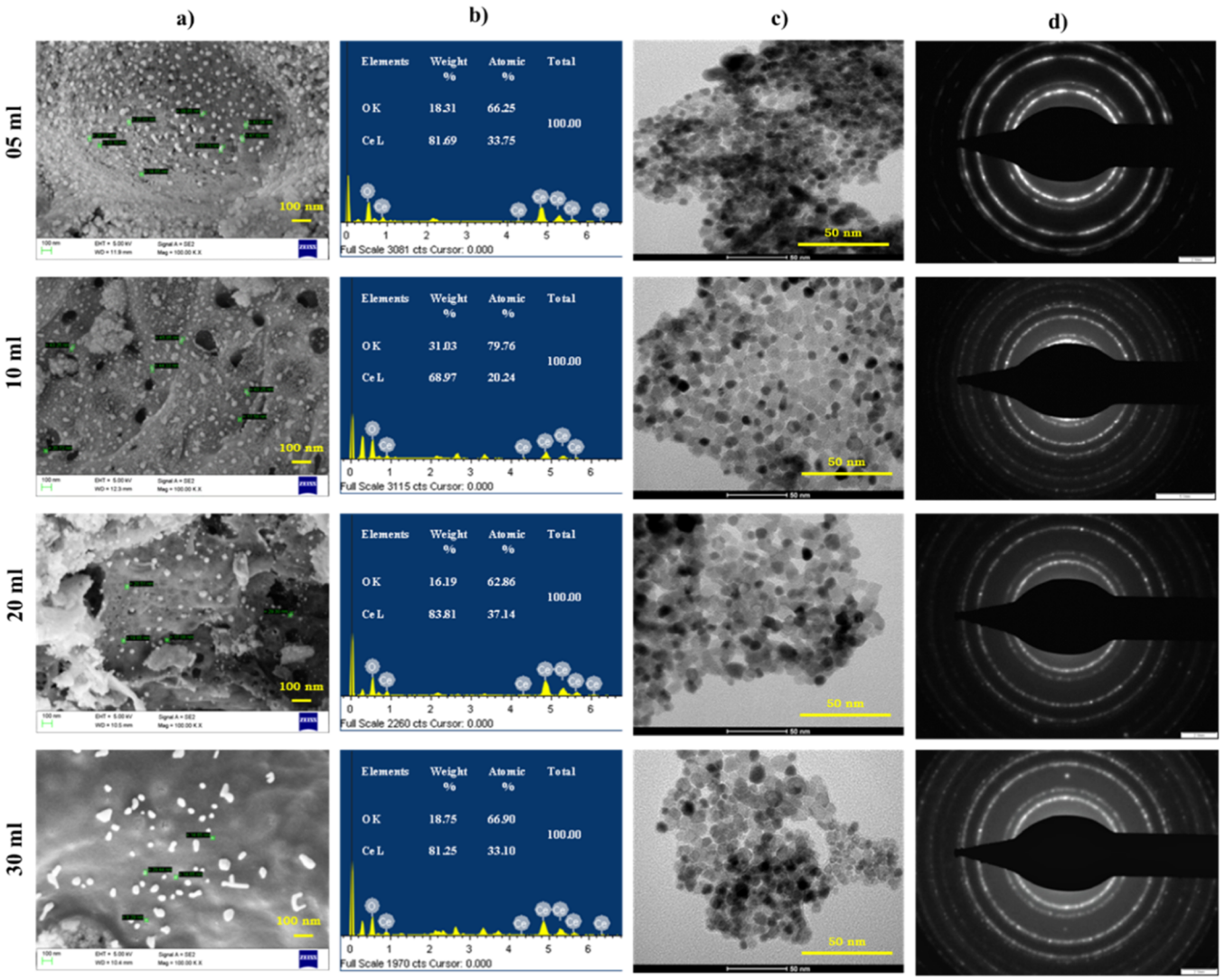

Figure 2. Morphology of CeO_2NPs synthesized using different volumes of *C. asiatica* extract. (a) SEM images, (b) EDX analysis, (c) HR-TEM images, and (d) SAED patterns.

10,000*g*. The unsolubilized DNPH was removed by washing the pellet with 1/1 ethyl acetate/ethanol twice by centrifuging for 5 min (3400*g*). Then, the pellet was suspended in 6 M guanidine hydrochloride (1.5 mL) in phosphate buffer of pH 6.5, and the absorbance was measured at 370 nm.

2.6.7.2. Evaluation of ROS Inhibition by Flow Cytometry. ROS inhibition was quantified by the method of Liu et al.[22] using a flow cytometer. The cell monolayer was washed and supplemented with fresh media and incubated for 2 h before the treatment. DCFH-DA solution (25 μM) was prepared in DMEM media, and 1 mL of this solution was poured into each well. After the solution was incubated for 45 min, the DCFH-DA solution was removed carefully. The cells were rinsed with 1× PBS once without disturbing the cell monolayer. The cells were treated with H_2O_2 (135 μM) for 24 h and then subjected to treatment with CeO_2NPs (20 and 40 μg/mL) for 24 h. 5 mM N-acetylcysteine (NAC) served as a positive control (ROS inhibitor). Post-incubation, the cells were processed for flow cytometry analysis by washing in 1× PBS and suspending the cells in sheath fluid. The fluorescent signal was then detected using the FL1H detector.

2.6.8. Apoptosis Analysis. 2.6.8.1. DAPI Staining. DAPI staining was done following the modified protocol of Lingappa et al.[23] The cells were treated as mentioned previously and fixed using 4% paraformaldehyde in PBS (10 min), followed by washing with PBS and staining with DAPI (1 μg/mL in PBS) for 20 min. After staining, the cells were observed under a confocal microscope (CKX41, Olympus Corporation, Japan). The apoptotic cells were identified using their condensed, fragmented, and degraded nuclei.

2.6.8.2. Apoptosis Detection Using PI and Annexin V-FITC by Flow Cytometry. Before apoptosis was introduced, the cells were cultured for 24 h. Pretreatment was done with 135 μM H_2O_2 for 24 h, and subsequent treatments with different concentrations (20 and 40 μg/mL) of biosynthesized CeO_2NPs for another 24 h were performed. Apoptosis was detected following the method of Zheng et al.[24] After treatment, the cells were processed and washed with cold PBS (twice), and then 1 mL of 1× binding buffer. 500 μL of the cell suspension was added with 10 and 5 μL of PI and annexin V, respectively, followed by incubation for 15 min in the dark at RT. Post incubation, the cells were subjected to flow cytometric analysis.

https://doi.org/10.1021/acsomega.3c07505
ACS Omega 2024, 9, 2639−2649

2.7. Statistical Analysis. The data is represented as mean ± SE. One-way analysis of variance (ANOVA) followed by Tukey's test was performed to analyze the antioxidant enzyme activities, markers of OS, and apoptosis. Probability values of less than 0.05 were statistically significant. The statistical analysis was carried out using a GraphPad prism.

3. RESULTS AND DISCUSSION

3.1. Characterization of CeO_2NPs. The prominent absorption peak observed at 304 nm confirms the formation of CeO_2NPs (Figure 1a). This peak may be attributed to the transfer of charge from the 2p valence band of O^{2-} to the Ce^{4+} 4f band.[25] The absorption band of the biosynthesized CeO_2 samples slightly shifts toward the lesser wavelength side, suggesting the higher bandgap in energy based on the vibrational frequencies of ions. CeO_2NPs exhibit strong absorption bands at 304 nm in the UV range, and no band of Ce (IV) in the visible region indicates the occurrence of a +3 ionic state of Ce ions. FTIR spectrum of CeO_2NPs showed several significant IR peaks in the range of 4000−400 cm^{-1}, as shown in Figure 1b. The spectra of the samples reveal a firm Ce metal−oxygen stretching band at about 512 cm^{-1}. The peaks at 3375.80 and 1622.71 cm^{-1} represent the hydroxyl stretch and water, respectively.

The phase formation and crystalline structure of the synthesized CeO_2NPs were studied using powder X-ray diffraction (PXRD) showing the patterns scanned at 2θ in the range of 10°−80° (Figure 1c). These profiles confirmed the polycrystalline nature and indicated the pure face-centered cubic phase structure. The peaks correspond to the crystal planes (111), (200), (220), (311), (222), and (400), which were well-matched with JCPDS no: 81-0792 of the CeO_2 cubic crystal group with space group $Fm\bar{3}m$ (225). In contrast, a slightly Ce_2O_3 hexagonal phase (JCPDS-74-1145) was observed when the *C. asiatica* extract was used for a few samples.

Scherer's formula was used to calculate the average crystallite size.[26] The average crystallite size and structural parameters are presented in Table S1. Observed broadening of the diffraction peaks in *C. asiatica*-extract-mediated samples indicates the reduction of crystallite sizes to nanoregime. The same was confirmed by HR-TEM analysis in the subsequent section. In order to validate the obtained PXRD data, a Rietveld refinement pattern was performed for CeO_2NPs prepared from a 20 mL *C. asiatica* extract sample using the FULLPROF program.[27] The refined parameters such as atomic functional positions and occupancy for the as-formed CeO_2NPs sample are tabulated in Table S2. Few peaks left out with error corresponded to the Ce_2O_3 of the hexagonal phase (JCPDS-74-1145) as an impurity observed in the prepared sample. The cubic structure of the synthesized CeO_2NPs was also confirmed by Raman spectroscopy (Figure 1d). The intense peak at 457 cm^{-1} confirms the Raman active F_{2g} mode of CeO_2, which may be due to the Ce−O8 vibrational symmetrical stretching mode.[28] More intense Raman peaks were observed in *C. asiatica*-mediated CeO_2 samples, and it became maximum for 5 mL and very close to the maximum for 20 mL of *C. asiatica* samples, indicating increased oxygen vacancies in these samples. The uniformity of the strain within each particle and the average strain formed by all the particles influence the position of the Raman line.[29] In the current study, the particle sizes were found to be uniform, and hence, collective strain emerging from all the particles is similar. Also, the peak asymmetries and shifting were not observed much due to a significantly less quantity of nonuniform strain contributed by most of the particles.

SEM microscopy at different magnification illustrates that the particles were uniform and spherical, and the mean size was less than 35 nm (Figure 2a). The EDX spectra of the synthesized CeO_2NPs indicate Ce and O elements and the high purity of the synthesized nanoceria (Figure 2b). The characterization result evidences the formation of CeO_2NPs, which had particle size in the nano regime and were pure in their chemical composition. SEM images showed (Figure 2a) an increase in porosity and slightly decreased particle size of the samples with an increase in the volume of the *C. asiatica* extract. The CeO_2NPs were agglomerated to form spherical-like clusters, with sizes ranging from micrometers to a few tenths of microns. The presence of agglomerated spherical clusters and numerous voids and pores seen in the samples may be due to the production of gases during solution combustion synthesis.[30]

The internal morphology of the sample (CeO_2NPs obtained using 20 mL *C. asiatica* extract) was characterized by HR-TEM and selected area electron diffraction (SAED). The HR-TEM image displayed spherical-shaped particles of ∼10 nm size (Figure 2c). The SAED pattern indicates several weak Scherrer rings conforming to the reflections of the cubic CeO_2 sample and also representing the high crystallinity of the NPs (Figure 2d). These reflection planes were in good accordance with PXRD results. HR-TEM images revealed the presence of 3.124 Å interplanar spacing, which correlated to the distance of the crystallographic cubic planes (111) of CeO_2 lattice fringes, suggesting the formation of high-quality cubic CeO_2NPs. HR-TEM analysis revealed a crystallite size of about 10 nm, which reasonably complies with the size estimated using the PXRD pattern by Scherrer's equation.

3.2. Antioxidant Assays. The free radical scavenging ability was evaluated by measuring the DPPH and hydroxyl radical activity. DPPH is a stable free radical and widely accepted method to determine an antioxidant compounds' free radical quenching ability.[31] The DPPH reduction was assessed by observing the decline in absorbance due to the formation of stable DPPH molecules. 10 mL of the prepared CeO_2NPs revealed significant dose-dependent activity, as apparent by its lesser IC_{50} value of 6.95 ± 1.16 μg/mL (Table 1). Our results are comparable with the reports of Nezhad et al.[32] wherein green synthesized CeO_2NPs significantly inhibited the free radicals.

The hydroxyl [OH] radical generated by the Fe^{2+} ions with a highly reactive oxygen center was estimated by the extent of

Table 1. DPPH and Hydroxyl Radical Scavenging Activities of CeO_2NPs Synthesized Using Different Volumes of *C. asiatica* Extract[a]

CeO_2 NPs synthesized using different volumes of extract	free radical scavenging activity (IC_{50} μg/mL)	OHDPPH
05 mL	09.21 ± 1.20[b]	21.75 ± 1.17
10 mL	06.95 ± 1.16	12.21 ± 1.19[b]
20 mL	11.26 ± 1.18[b]	11.23 ± 1.20
30 mL	11.82 ± 1.36[b]	17.93 ± 1.15
Vit C	03.99 ± 1.76	20.37 ± 1.16

[a]The data is analyzed by one-way ANOVA and expressed as mean ± standard error (SE) from three independent experiments. [b]$p < 0.05$, samples compared with vitamin C.

https://doi.org/10.1021/acsomega.3c07505
ACS Omega 2024, 9, 2639−2649

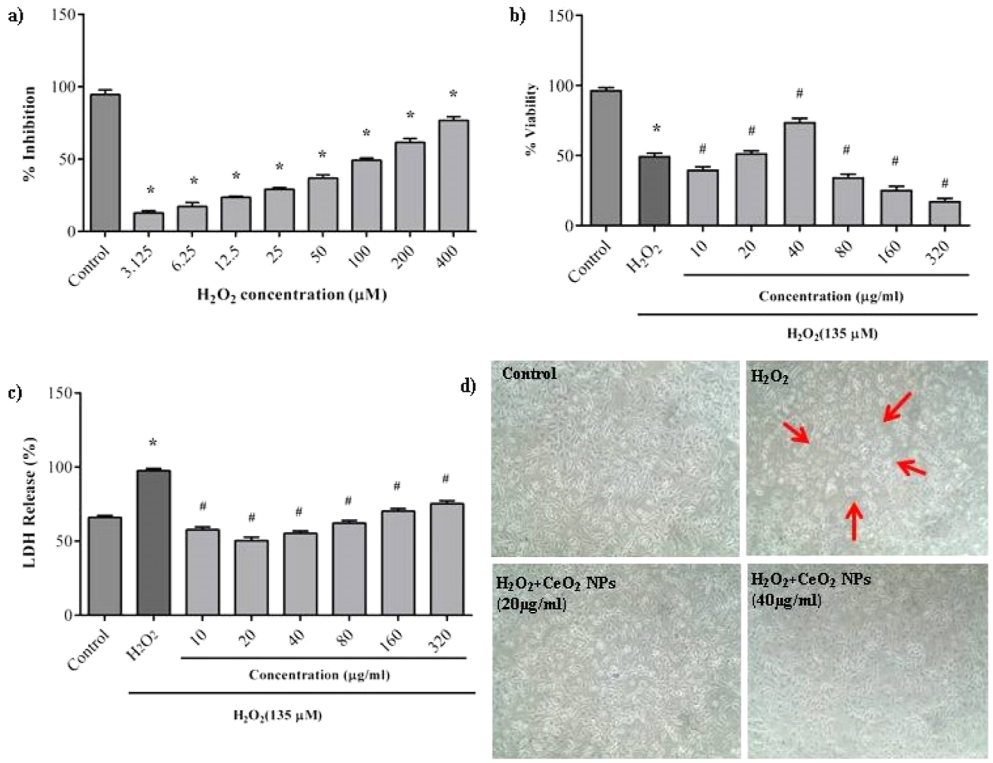

Figure 3. Effects of CeO_2NPs on H_2O_2-induced cytotoxicity in SH-SY5Y cells. (a) Cells treated with varying concentration of H_2O_2 (3.125−400 μg/mL) for 24 h. (b) Cells pretreated with H_2O_2 followed by incubation with CeO_2NPs for 24 h, and cell viability was determined by MTT assay. (c) Cells pretreated with H_2O_2 followed by incubation with CeO_2NPs for 24 h, and cell cytotoxicity was measured by LDH assay. (d) Morphology of SH-SY5Y cells observed under phase contrast microscope. The data is expressed as mean ± SE from three independent experiments and analyzed by one-way ANOVA followed by Tukey's test. *$p < 0.05$ significance compared with control; #$p < 0.05$ significance compared with H_2O_2-treated cells.

deoxyribose degradation.[33] As depicted in Table 1, a remarkable feature in OH radical activity is that the CeO_2NPs prepared with 10 and 20 mL of plant extract exhibited higher inhibitory activity (12.21 ± 1.19 and 11.23 ± 1.20 μg/mL) compared to that of vitamin C. The antioxidant properties of CeO_2NPs are attributable to the greater oxygen vacancy that enhances its reactivity leading to higher radical scavenging ability.[34]

3.3. In Vitro Studies. *3.3.1. Dose Fixation.* CeO_2NPs synthesized using different volumes of plant extract (5, 10, 20, and 30 mL) were screened to determine the neuroprotective activity against OS induced by H_2O_2 in SH-SY5Y cells. The effective volume of plant-extract-synthesized CeO_2NPs was assessed based on the MTT, LDH, and the levels of antioxidant enzyme activities and protein oxidation. 20 mL of prepared CeO_2NPs was most effective in neuroprotective activity and enhanced antioxidant status. Hence, 20 mL of prepared CeO_2NPs was selected for further studies.

3.3.2. Effect of H_2O_2 on Cell Viability through MTT Assay. H_2O_2 is one of the most potent inducers of OS by producing highly reactive OH radicals through the Fenton reaction.[35] H_2O_2 is a physiologically and pathologically significant cytotoxicant that can quickly diffuse through the plasma membrane.[36] MTT assay, which is a sensitive and reliable indicator of the cells' metabolic activity, was used to determine the viability of the SH-SY5Y cells upon H_2O_2-induced OS. This assay is based on the capacity of functional mitochondria to convert MTT dye into formazan crystals.[37,38] As evident from Figure 3, the SH-SY5Y cells exhibited dose-dependent cytotoxicity upon treatment with various concentrations of H_2O_2 (3.125−400 μM) with an IC_{50} value of 135 μM. Hence, this concentration was fixed to assess the protective activity of CeO_2NPs against H_2O_2 exposure in further experiments.

3.3.3. Effect of Synthesized CeO_2NPs against H_2O_2-Induced Cytotoxicity. To evaluate the cytoprotective ability of CeO_2NPs on H_2O_2-mediated cytotoxicity, the SH-SY5Y cells were treated with varying concentrations of CeO_2NPs for 24 h after exposure to H_2O_2. As shown in Figure 3a, the H_2O_2-treated cells significantly decreased cell viability. However, treatment of CeO_2NPs at 20, and 40 μg/mL remarkably attenuated H_2O_2-induced cytotoxicity by 74.44% and 51.77% over the control cells. The higher doses of CeO_2NPs reduced the cell viability of the H_2O_2-exposed cells (Figure 3b). We further examined the levels of LDH leakage, which is an important marker of the membrane integrity and cell death. Our results (Figure 3c) revealed higher LDH leakage in H_2O_2-treated cells. However, treatment with 20 and 40 μg/mL of CeO_2NPs significantly reduced the LDH leakage (50.45% and 55.45%) over cells treated with H_2O_2 alone.

The morphological observations also supported the protective effects of CeO_2NPs. H_2O_2-exposed cells showed irregular shape, membrane blebbing, detachment, shrinkage, and higher cell mortality. Meanwhile, treatment with CeO_2NPs prevented these morphological changes, depicting the neuroprotective activity of CeO_2NPs against H_2O_2-mediated cytotoxicity (Figure 3d).

3.3.4. Cellular Uptake Studies. Cellular uptake of CeO_2NPs in the SH-SY5Y cells was studied using flow cytometry analysis based on SSC signals. The CeO_2NPs were internalized within 24 h of exposure in a concentration-dependent manner, as

https://doi.org/10.1021/acsomega.3c07505
ACS Omega 2024, 9, 2639−2649

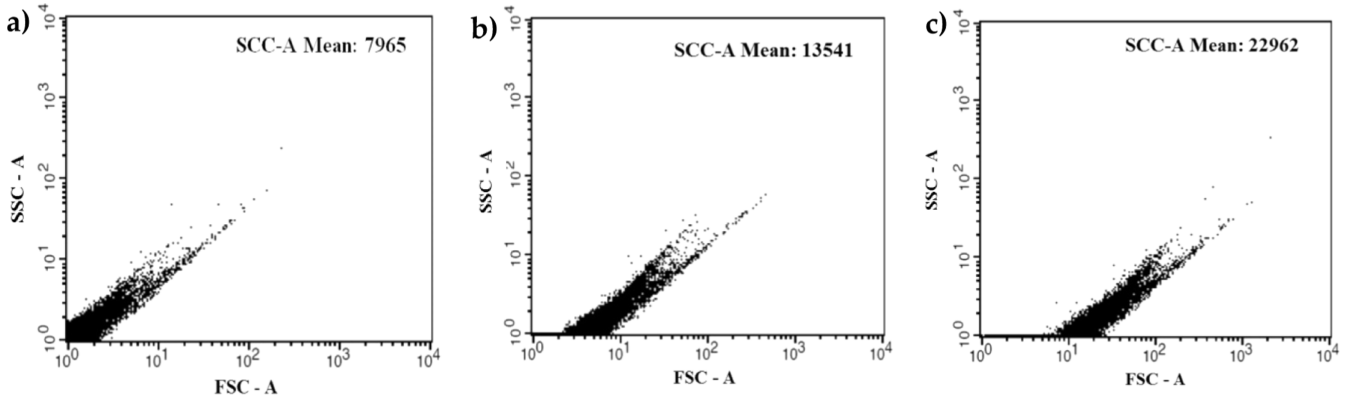

Figure 4. Cellular uptake of CeO_2NPs in SH-SY5Y cells. (a) Control, (b) CeO_2NPs (20 μg/mL), and (c) CeO_2NPs (40 μg/mL).

indicated by increasing SSC intensity compared to that of control cells. As shown in Figure 4, the maximum uptake of CeO_2NPs was found at 40 μg/mL (22,962). The increase in SSC intensity indicates the increased cell density, which can be correlated to the successful uptake of CeO_2NPs in the SH-SY5Y cells. Our findings were in accordance with the studies of Patel et al.[39]

3.3.5. Antioxidant Enzyme Activities. SOD, CAT, and GPx are the first lines of an antioxidant defense system. These enzymes protect the cells by scavenging free radicals produced by various biochemical reactions in the body, thereby making less toxic metabolites and inhibiting OS.[40,41] To evaluate the antioxidant ability of nanoceria, we assessed the SOD, CAT, and GPx activities. Our results revealed diminished antioxidant enzyme activity in H_2O_2-treated cells with respect to control, which might be due to the increased generation of ROS. However, a prominent increase in the enzymatic activity was seen in the CeO_2NP-treated cells compared to that in H_2O_2-treated cells. The maximum activity was noticed in 20 μg/mL synthesized CeO_2NPs [SOD (63.92%), CAT (72.36%), and GPx (34.68%)] as depicted in Figure 5. The upregulation of the enzyme activities is attributable to the transition capacity of phytosynthesized NPs to switch between Ce^{3+} and Ce^{4+} ions, which mimic SOD, CAT, and peroxidase activity.[42]

3.3.6. Markers of OS. 3.3.6.1. Determination of PC Content. PCs, an important biomarker of protein oxidation, significantly increased by 11.92% in H_2O_2-treated cells. The treatment of CeO_2NPs markedly attenuated the PC content, with a maximum decrease seen in 20 μg/mL CeO_2NP-treated cells (4.82%) compared to that in H_2O_2-treated cells (Figure 6). The reduction in protein carbonyl levels can be accredited to the excellent antioxidant properties of CeO_2NPs, which are in line with the studies of Soren et al.[43] and Arya et al.[44]

3.3.6.2. Intracellular ROS Measurement. To determine the protective activity of CeO_2NPs on H_2O_2-induced ROS generation, we utilized a cell-permeable DCFH-DA fluorescent probe. As shown in Figure 7, ROS generation significantly increased in H_2O_2-treated cells (58.27%) compared to that in control. The elevated ROS levels induced by H_2O_2 were attenuated considerably in CeO_2NP-treated SH-SY5Y cells, suggesting the efficient scavenging ability of CeO_2NPs in preventing OS.

3.3.7. Apoptotic Analysis. Apoptosis is a means of regulating cell death, which is crucial for cellular homeostasis. It is marked by nuclear changes leading to the formation of apoptotic bodies and cell death.[45] The protective effect of CeO_2NPs on H_2O_2-induced apoptosis was determined by

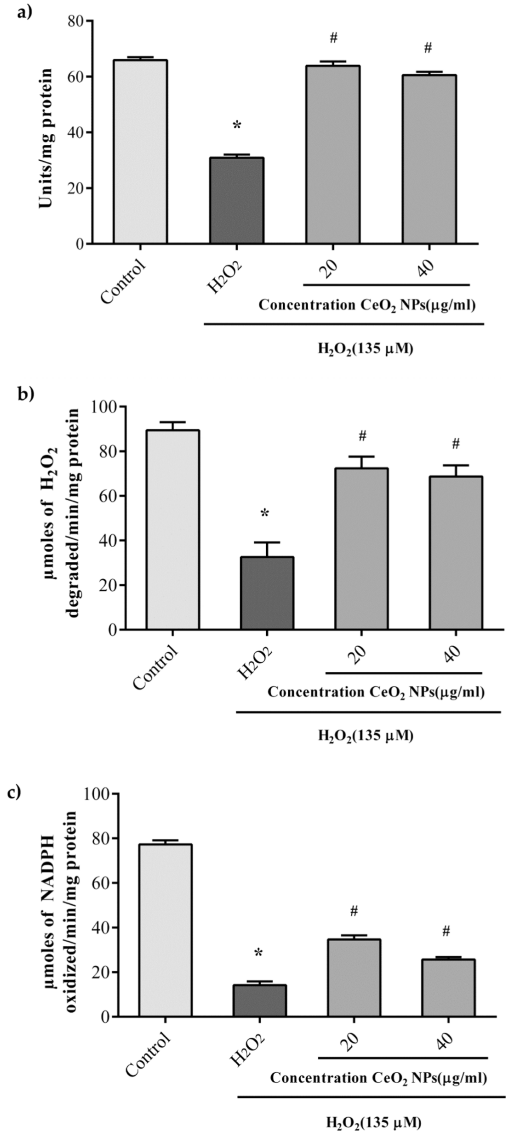

Figure 5. Effect of CeO_2NPs on antioxidant enzyme activities in H_2O_2-treated cells: (a) SOD, (b) CAT, and (c) GPx. The data is analyzed from three independent experiments by one-way ANOVA followed by Tukey's test. *p < 0.05 significance compared with control; #p < 0.05 significance compared with H_2O_2-treated cells.

DAPI staining. As shown in Figure 8, the H_2O_2-treated cells showed distinct apoptotic characteristics such as chromatin

https://doi.org/10.1021/acsomega.3c07505
ACS Omega 2024, 9, 2639−2649

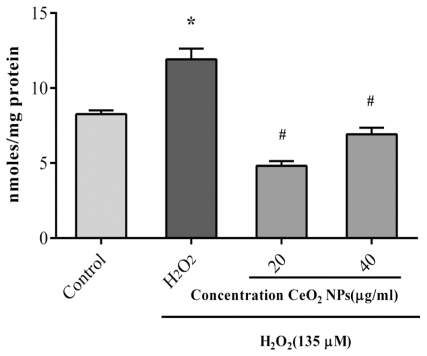

Figure 6. Effect of CeO_2NPs on PC levels in H_2O_2-treated SH-SY5Y cells. The data is analyzed from three independent experiments by one-way ANOVA followed by Tukey's test. *p < 0.05 significance compared with control; #p < 0.05 significance compared with H_2O_2-treated cells.

condensation, nuclear fragmentation, and cell shrinkage. The treatment of cells with CeO_2NPs drastically decreased the number of apoptotic cells. Annexin-V-FITC/PI costaining was further carried out to estimate the apoptosis through flow cytometric analysis quantitatively. The apoptotic rate in the H_2O_2-treated cells increased from 5.74% to 64% compared with that of the control. Interestingly, treatment of 20 and 40 μg/mL of CeO_2NPs remarkably attenuated SH-SY5Y cell apoptosis by 31% and 44%, respectively (Figure 8).

4. CONCLUSIONS

The green synthesis of CeO_2NPs using *C. asiatica* leaf extract is a simple, rapid, and eco-friendly method. The UV−vis, XRD, FTIR, SEM−EDAX, and HR-TEM analyses confirm the nanoregime purity, crystallite structures, size, morphology, and optical properties. The synthesized NPs exhibited excellent free radical scavenging activity against DPPH and OH radicals. Our results revealed that CeO_2NPs might protect the SH-SY5Y cells against OS induced by H_2O_2 by modulating antioxidant status and apoptosis due to effective redox switching in nanoscale. These findings suggest that CeO_2NPs may be a potential therapeutic agent for treating OS-related neurodegenerative disorders. However, further studies must be performed to ascertain its role in nanomedicine.

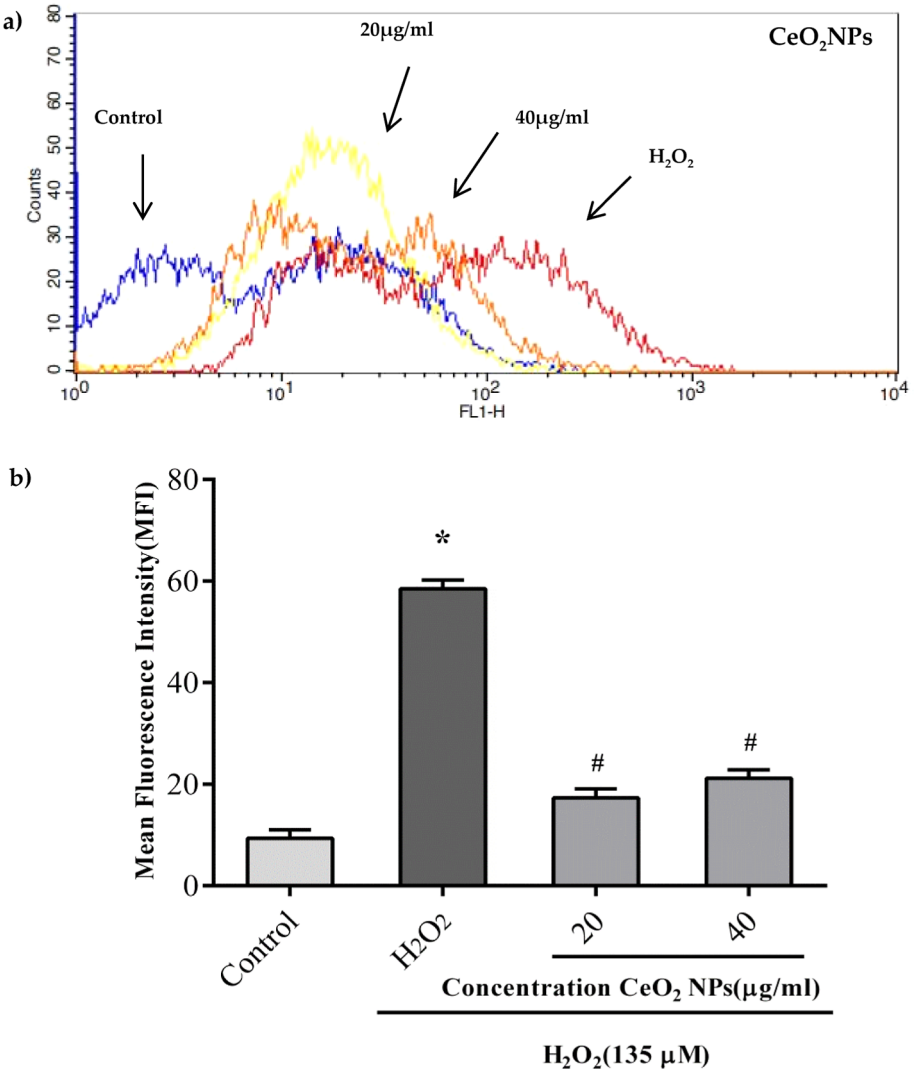

Figure 7. Effect of CeO_2NPs on ROS generation in H_2O_2-treated SH-SY5Y cells. (a) ROS determination by flow cytometry. (b) Quantitative analysis of the ROS fluorescence intensity. The data is analyzed from three independent experiments by one-way ANOVA followed by Tukey's test. *p < 0.05 significance compared with control; #p < 0.05 significance compared with H_2O_2-treated cells.

https://doi.org/10.1021/acsomega.3c07505
ACS Omega 2024, 9, 2639−2649

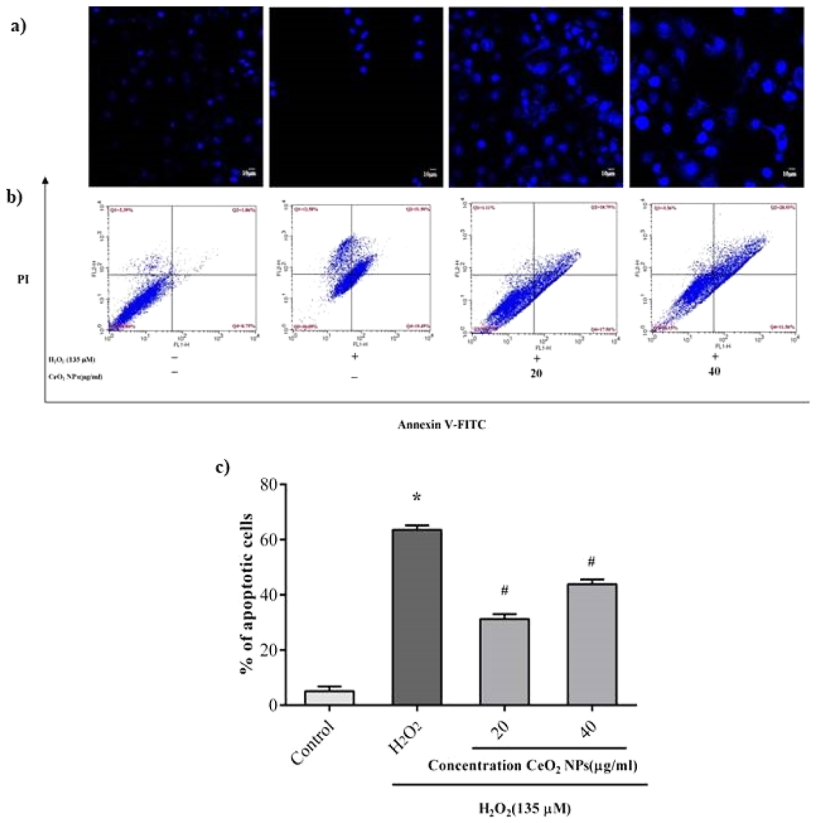

Figure 8. Effect of CeO_2NPs on H_2O_2-induced apoptosis in SH-SYSY cells. (a) Morphology of cell nucleus using DAPI staining. (b) Flow cytometry. (c) Percentage of apoptotic cells. Data were expressed as mean ± SE (n = 3). Statistical analysis was performed by t-test. *p < 0.05 significance compared with control; #p < 0.05 compared with H_2O_2-treated cells.

■ ASSOCIATED CONTENT

Data Availability Statement

Data is included within the article and in the Supporting Information.

Supporting Information

The Supporting Information is available free of charge at https://pubs.acs.org/doi/10.1021/acsomega.3c07505.

Various structural parameters of CeO2 NPs and Rietveld refined data for the CeO_2NPs obtained using *C. asiatica* extract (PDF)

■ AUTHOR INFORMATION

Corresponding Authors

Mohammad Azam Ansari − *Department of Epidemic Disease Research, Institutes for Research and Medical Consultations (IRMC), Imam, Abdulrahman Bin Faisal University, Dammam 31441, Saudi Arabia;* orcid.org/0000-0002-6122-5479; Email: maansari@iau.edu.sa

Thimappa Ramachandrappa Lakshmeesha − *Department of Microbiology and Biotechnology, Bangalore University, Bengaluru 560056 Karnataka, India;* Email: lakshmeeshat6@gmail.com

Tekupalli Ravikiran − *Department of Microbiology and Biotechnology, Bangalore University, Bengaluru 560056 Karnataka, India;* Email: ravikiran@bub.ernet.in

Authors

Madhugiri Gopinath Mamatha − *Department of Microbiology and Biotechnology, Bangalore University, Bengaluru 560056 Karnataka, India*

M Yasmin Begum − *Department of Pharmaceutics, College of Pharmacy, King Khalid University, Abha 61421, Saudi Arabia*

Daruka Prasad B. − *Department of Physics, B.M.S. Institute of Technology, Bengaluru 560064 Karnataka, India;* orcid.org/0000-0002-6485-3673

Adel Al Fatease − *Department of Pharmaceutics, College of Pharmacy, King Khalid University, Abha 61421, Saudi Arabia*

Umme Hani − *Department of Pharmaceutics, College of Pharmacy, King Khalid University, Abha 61421, Saudi Arabia*

Mohammad N. Alomary − *Advanced Diagnostic and Therapeutic Institute, King Abdulaziz City for Science and Technology (KACST), Riyadh 11442, Saudi Arabia*

Sumreen Sultana − *Department of Microbiology and Biotechnology, Bangalore University, Bengaluru 560056 Karnataka, India;* orcid.org/0000-0001-7771-3461

Shital Manohar Punekar − *Department of Microbiology and Biotechnology, Bangalore University, Bengaluru 560056 Karnataka, India*

Nivedika M.B. − *Department of Microbiology and Biotechnology, Bangalore University, Bengaluru 560056 Karnataka, India*

Complete contact information is available at: https://pubs.acs.org/10.1021/acsomega.3c07505

Notes

The authors declare no competing financial interest.

https://doi.org/10.1021/acsomega.3c07505
ACS Omega 2024, 9, 2639−2649

Ethical Approval: This study does not contain any work related to human participants or animals performed by any of the authors.

■ ACKNOWLEDGMENTS

The authors extend their appreciation to the Deanship of Scientific Research at King Khalid University for funding this work through Large Group Reserach Project under grant number RGP2/54/44. This work was supported by Bangalore University Research Promotion Board. We wish to thank the Department of Microbiology and Biotechnology for providing infrastructural facilities.

■ REFERENCES

(1) Kim, S. Y.; Park, C.; Jang, H. J.; Kim, B. o.; Bae, H. W.; Chung, I. Y.; Kim, E. S.; Cho, Y. H. Antibacterial strategies inspired by the oxidative stress and response networks. *J. Microbio.* **2019**, *57*, 203−212.

(2) Sowbhagya, R.; Anupama, S. K.; Bhagyalakshmi, D.; et al. Modulatory effects of decalepis hamiltonii extract and its compounds on the antioxidant status of the aging rat brain. *J. Pharm. Bioallied. Sci.* **2017**, *9*, 8.

(3) Capek, J.; Rousar, T. Detection of oxidative stress induced by nanomaterials in cells—the roles of reactive oxygen species and glutathione. *Molecules* **2021**, *26* (16), 4710.

(4) Naz, S.; Beach, J.; Heckert, B.; Tummala, T.; Pashchenko, O.; Banerjee, T.; Santra, S. Cerium oxide nanoparticles: A "radical" approach to neurodegenerative disease treatment. *Nanomedicine* **2017**, *12*, 545−553.

(5) Ranjbar, A.; Soleimani Asl, S.; Firozian, F.; Heidary Dartoti, H.; Seyedabadi, S.; Taheri Azandariani, M.; Ganji, M. Role of cerium oxide nanoparticles in a paraquat-induced model of oxidative stress: emergence of neuroprotective results in the brain. *J. Mol. Neurosci.* **2018**, *66*, 420−427.

(6) Najafi, R.; Hosseini, A.; Ghaznavi, H.; Mehrzadi, S.; Sharifi, A. M. Neuroprotective effect of cerium oxide nanoparticles in a rat model of experimental diabetic neuropathy. *Brain Res. Bull.* **2017**, *131*, 117−122.

(7) Vinothkumar, G.; Arunkumar, P.; Mahesh, A.; Dhayalan, A.; Suresh Babu, K. Size-and defect-controlled anti-oxidant enzyme mimetic and radical scavenging properties of cerium oxide nanoparticles. *New J. Chem.* **2018**, *42*, 18810−18823.

(8) Nyoka, M.; Choonara, Y. E.; Kumar, P.; Kondiah, P. P. D.; Pillay, V. Synthesis of cerium oxide nanoparticles using various methods: implications for biomedical applications. *Nanomaterials* **2020**, *10* (2), 242.

(9) Jeevitha, M.; Ravi, P. V.; Subramaniyam, V.; Pichumani, M.; Sripathi, S. K. Exploring the phyto-and physicochemical evaluation, fluorescence characteristics, and antioxidant activities of Acacia ferruginea Dc: an endangered medicinal plant. *Fut. J. Pharma. Sci.* **2021**, *7*, 228.

(10) Thong-on, W.; Pathomwichaiwat, T.; Boonsith, S.; Koo-amornpattana, W.; Prathanturarug, S. Green extraction optimization of triterpenoid glycoside-enriched extract from centella asiatica (L.) urban using response surface methodology (RSM). *Sci. Rep.* **2021**, *11*, 22026.

(11) Jhansi, D.; Kola, M. The antioxidant potential of centella asiatica: A review. *J. Med. Plants. Stud.* **2019**, *7*, 18−20.

(12) Lakshmeesha, T. R.; Kalagatur, N. K.; Mudili, V.; Mohan, C. D.; Rangappa, S.; Prasad, B. D.; Ashwini, B. S.; Hashem, A.; Alqarawi, A. A.; Malik, J. A.; et al. Biofabrication of zinc oxide nanoparticles with Syzygium aromaticum flower buds extract and finding its novel application in controlling the growth and mycotoxins of Fusarium graminearum. *Front. Microbiol.* **2019**, *10*, 1244.

(13) Ravikiran, T.; Anand, S.; Ansari, M. A.; Alomary, M. N.; AlYahya, S.; Ramachandregowda, S.; Alghamdi, S.; Sindhghatta Kariyappa, A.; Dundaiah, B.; Madhugiri Gopinath, M.; et al. Fabrication and in vitro Evaluation of 4-HIA Encapsulated PLGA Nanoparticles on PC12 Cells. *Int. J. Nanomed.* **2021**, *16*, 5621−5632.

(14) Halliwell, B.; Gutteridge, J. M. C. Formation of a thiobarbituric-acid-reactive substance from deoxyribose in the presence of iron salts. The role of superoxide and hydroxyl radicals. *FEBS Lett.* **1981**, *128*, 347−352.

(15) Mosmann, T. Rapid colorimetric assay for cellular growth and survival: Application to proliferation and cytotoxicity assays. *J. Immunol. Methods* **1983**, *65*, 55−63.

(16) Chauhan, D.; Sri, S.; Kumar, R.; Panda, A. K.; Solanki, P. R. Evaluation of size, shape, and charge effect on the biological interaction and cellular uptake of cerium oxide nanostructures. *Nanotechnology* **2021**, *32* (35), 355101.

(17) Lowry, O. H.; Rosenberg, N. J.; Farr, A. I.; et al. Protein measurements with the Folin phenol reagent. *J. Biol. Chem.* **1951**, *100*, 201−220.

(18) Misra, H. P.; Fridovich, I. The role of superoxide anion in the autoxidation of epinephrine and a simple assay for superoxide dismutase. *J. Biol. Chem.* **1972**, *247*, 3170−3175.

(19) Aebi, H. [13] Catalase in Vitro. *Methods Enzymol.* **1984**, *105*, 121−126.

(20) Flohe, L.; Gunzler, W. A. [12] Assays of glutathione peroxidase. *Methods Enzymol.* **1984**, *105*, 114−120.

(21) Levine, R. L.; Williams, J. A.; Stadtman, E. P.; Shacter, E. Carbonyl assays for determination of oxidatively modified proteins. *Methods Enzymol.* **1994**, *233*, 346−357.

(22) Liu, T. I.; Lu, T. Y.; Yang, Y. C.; Chang, S. H.; Chen, H. H.; Lu, I. L.; Sabu, A.; Chiu, H. C. New combination treatment from ROS-Induced sensitized radiotherapy with nanophototherapeutics to fully eradicate orthotopic breast cancer and inhibit metastasis. *Biomaterials* **2020**, *257*, 120229.

(23) Lingappa, S.; Shivakumar, M. S.; Manivasagam, T.; Somasundaram, S. T.; Seedevi, P. Neuroprotective effect of epalrestat on hydrogen peroxide-induced neurodegeneration in SH-SY5Y cellular model. *J. Microbiol. Biotechnol.* **2021**, *31*, 867−874.

(24) Zheng, C.; Zhou, M.; Sun, J.; Xiong, H.; Peng, P.; Gu, Z.; Deng, Y. The protective effects of liraglutide on AD-like neurodegeneration induced by oxidative stress in human neuroblastoma SH-SY5Ycells. *Chem.-Biol. Interact.* **2019**, *310*, 108688.

(25) Portillo, M. C.; Moreno, O. P.; Mora-Ramirez, M. A.; Santiesteban, H. J.; Avendaño, C. B.; Bernal, Y. P. Optical and structural analysis of the charge transfer of Ce3++ e-→ Ce4+ ion in the cerium oxide (CeO2). *Optik* **2021**, *248*, 168178.

(26) Valeur, B.; Berberan-Santos, M. N. A brief history of fluorescence and phosphorescence before the emergence of quantum theory. *J. Chem. Educ.* **2011**, *88*, 731−738.

(27) Wyckoff, R. Interscience publishers, new york, new York rocksalt structure. *Cryst. Struc.* **1963**, *1*, 85−237.

(28) Suzuki, T.; Kosacki, I.; Anderson, H. U.; Colomban, P. Electrical conductivity and lattice defects in nanocrystalline cerium oxide thin films. *J. Am. Ceram. Soc.* **2001**, *84*, 2007−2014.

(29) Spanier, J. E.; Robinson, R. D.; Zhang, F.; Chan, S. W.; Herman, I. P. Size-dependent properties of CeO2-y nanoparticles as studied by Raman scattering. *Phys. Rev. B* **2001**, *64*, 245407.

(30) Vidya, Y. S.; Anantharaju, K. S.; Nagabhushana, H.; Sharma, S.; Nagaswarupa, H.; Prashantha, S.; Shivakumara, C.; Danithkumar. Combustion synthesized tetragonal ZrO2: Eu3+ nanophosphors: structural and photoluminescence studies. *Spectrochim. Acta, Part A* **2015**, *135*, 241−251.

(31) Romanet, R.; Coelho, C.; Liu, Y.; Bahut, F.; Ballester, J.; Nikolantonaki, M.; Gougeon, R. The antioxidant potential of white wines relies on the chemistry of sulfur-containing compounds: An optimized DPPH assay. *Molecules* **2019**, *24*, 1353.

(32) Nezhad, A. S.; Es-haghi, A.; Tabrizi, M. H. Green synthesis of cerium oxide nanoparticle using origanum majorana l. leaf extract, its characterization and biological activities. *Appl. Organomet. Chem.* **2020**, *34*, No. e5314.

(33) Muthuvel, A.; Jothibas, M.; Mohana, V.; Manoharan, C. Green synthesis of cerium oxide nanoparticles using calotropis procera

https://doi.org/10.1021/acsomega.3c07505
ACS Omega 2024, 9, 2639−2649

flower extract and their photocatalytic degradation and antibacterial activity. *Inorg. Chem. Commun.* **2020**, *119*, 108086.
(34) Saikia, H.; Hazarika, K. K.; Chutia, B.; Choudhury, B.; Bharali, P. A simple chemical route toward high surface area CeO2 nanoparticles displaying remarkable radical scavenging activity. *Chem. Sel.* **2017**, *2*, 3369−3375.
(35) Anupama, S. K.; Sowbhagya, R.; Bhagyalakshmi, D.; Vijay, K.; Ravikiran, T. Decalepis hamiltonii protects H9C2 Cells against H2O2 induced oxidative stress and apoptosis through modulating anti-oxidant status. *Med. Plants* **2019**, *11*, 87−94.
(36) Tabernilla, A.; dos Santos Rodrigues, B.; Pieters, A.; Caufriez, A.; Leroy, K.; Van Campenhout, R.; Cooreman, A.; Gomes, A. R.; Arnesdotter, E.; Gijbels, E.; et al. In vitro liver toxicity testing of chemicals: A pragmatic approach. *Int. J. Mol. Sci.* **2021**, *22*, 5038.
(37) Sangsefidi, F. S.; Nejati, M.; Verdi, J.; Salavati-Niasari, M. Green synthesis and characterization of cerium oxide nanostructures in the presence carbohydrate sugars as a capping agent and investigation of their cytotoxicity on the mesenchymal stem cell. *J. Clean. Prod.* **2017**, *156*, 741−749.
(38) Miri, A.; Sarani, M.; Khatami, M. Nickel-doped cerium oxide nanoparticles: biosynthesis, cytotoxicity and UV protection studies. *RSC Adv.* **2020**, *10*, 3967−3977.
(39) Patel, P.; Kansara, K.; Singh, R.; Shukla, R. K.; Singh, S.; Dhawan, A.; Kumar, A. Cellular internalization and antioxidant activity of cerium oxide nanoparticles in human monocytic leukemia cells. *Int. J. Nanomed.* **2018**, *13*, 39−41.
(40) Adebayo, O. A.; Akinloye, O.; Adaramoye, O. A. Cerium oxide nanoparticles attenuate oxidative stress and inflammation in the liver of diethylnitrosamine-treated mice. *Biol. Trace Elem. Res.* **2020**, *193*, 214−225.
(41) Pardhiya, S.; Priyadarshini, E.; Rajamani, P. In vitro antioxidant activity of synthesized BSA conjugated manganese dioxide nano-particles. *SN Appl. Sci.* **2020**, *2*, 1597.
(42) Yadav, N.; Singh, S. SOD mimetic cerium oxide nanorods protect human hepatocytes from oxidative stress. *Emergent Mater.* **2021**, *4*, 1305−1317.
(43) Soren, S.; Jena, S. R.; Samanta, L.; Parhi, P. Antioxidant Potential and Toxicity Study of the cerium oxide nanoparticles synthesized by microwave-mediated synthesis. *Appl. Biochem. Biotechnol.* **2015**, *177*, 148−161.
(44) Arya, A.; Gangwar, A.; Singh, S. K.; et al. Cerium oxide nanoparticles promote neurogenesis and abrogate hypoxia-induced memory impairment through AMPK-PKC-CBP signaling cascade. *Int. J. Nanomed.* **2016**, *11*, 1159−1173.
(45) Datta, A.; Mishra, S.; Manna, K.; Saha, K. D.; Mukherjee, S.; Roy, S. Pro-oxidant therapeutic activities of cerium oxide nano-particles in colorectal carcinoma cells. *ACS Omega* **2020**, *5*, 9714−9723.

https://doi.org/10.1021/acsomega.3c07505
ACS Omega 2024, 9, 2639−2649